Journal of Applied Polymer Science

Preparation and Characterization of Cerium-Doped Titanium Dioxide/Ultrahigh-Molecular-Weight Polyethylene Porous Composites with Excellent Photocatalytic Activity

Lixiu Gong,[1] Zhufa Zhou,[1,2] Shumei Wang,[1,2] Ben Wang[1]

[1]College of Chemistry, Chemical Engineering and Materials Science, Soochow University, Suzhou 215123, People's Republic of China

[2]National Engineering Laboratory of Modern Silk, Soochow University, Suzhou 215123, People's Republic of China

Correspondence to: Z. Zhou (E-mail: zhouzhufa@suda.edu.cn)

ABSTRACT: Porous ultrahigh-molecular-weight polyethylene (UHMWPE)-based composites filled with surface-modified Ce-doped TiO_2 nanoparticles (Ce–TiO_2/UHMWPE) were prepared by template dissolution. The composites were characterized by Fourier transform infrared spectroscopy, ultraviolet (UV)–visible spectroscopy, diffuse reflectance spectra, and scanning electron microscopy); the photocatalytic activity was also evaluated by the decomposition of methyl orange under UV exposure. The results demonstrate that the severe aggregation of Ce–TiO_2 nanoparticles could be reduced by surface modification via a silane coupling agent (KH570). The Ce–TiO_2/UHMWPE porous composites exhibited a uniform pore size. Doping with Ce^{4+} effectively extended the spectral response from the UV to the visible region and enhanced the surface hydroxyl groups of the TiO_2 attached to the matrix. With a degradation rate of 85.3%, the 1.5 vol % Ce–TiO_2/UHMWPE sample showed the best photocatalytic activity. The excellent permeability of the porous composites is encouraging for their possible use in wastewater treatment. © 2012 Wiley Periodicals, Inc. J. Appl. Polym. Sci. 129: 1212–1217, 2013

KEYWORDS: catalysts; composites; porous materials

Received 9 September 2012; accepted 14 October 2012; published online 27 November 2012
DOI: 10.1002/app.38728

INTRODUCTION

Porous polymeric materials play important roles in many fields, especially in the treatment of industry wastewater.[1–3] Among all polymer materials, ultrahigh-molecular-weight polyethylene (UHMWPE) has been considered a type of engineering plastic with many outstanding properties, including excellent mechanical properties, thermal stability, and corrosion resistance.[4–6] These features make UHMWPE a good candidate as a porous material for use in the separation processes. However, because of its hydrophobic characteristics, an apparatus fabricated from UHMWPE can be susceptible to contamination by impurities in the procedure of wastewater treatment; this affects the flux and limits its application. Therefore, the modification of UHMWPE porous materials is necessary. Many methods, including physical blending, chemical grafting, and periodic cleaning,[7–9] have been applied to improve the hydrophilicity of polymeric porous materials. However, these approaches increase the manufacturing costs and are limited by the fact that hydrophilic modification occurs only on the surface of the porous material, whereas the internal pores remain inclined to fouling. If the hydrophilicity of both the internal and external surfaces of a porous material is increased with a suitable method, the fouling will be remarkably reduced, and hence, the separation efficiency will be increases.

TiO_2 in different forms can effectively degrade various pollutants under UV irradiation.[10–12] Hence, many studies have been done to disperse TiO_2 in the polymer matrix to improve the antifouling properties and hydrophilicity.[13–16] However, the band gap of TiO_2 (3.2 eV for anatase) is too wide to absorb other lights, except for UV light.[17,18] Many approaches have been developed to extend the response range of TiO_2.[19–21] Among these methods, rare-earth-ion-doped TiO_2 has become a hotspot because it not only can extend the photoresponse in the visible regions but also can exist as a trap to separate electron–hole pairs under light irradiation. Anyway, the presence of ceria at the anatase surface can enhance the photodegradation without changing the properties of the polymer matrix.[22]

In this work, our aim was to prepare porous Ce–TiO_2/UHMWPE materials with remarkable permeabilities, enhanced hydrophilicities, and a wide photoresponse region for the self-cleaning properties. The Ce–TiO_2/UHMWPE porous composites

Table I. Specifications of the Samples with Different Concentrations of Ce in 5 vol % Ce–TiO_2

Porous material	Molar proportion of Ce in TiO_2 (mol %)
C_0	0
C_1	0.5
C_2	1.0
C_3	1.5
C_4	2.0
C_5	2.5

were obtained via template dissolution. The optical properties, thermal stability, and surface morphology of the composites were systematically investigated. In addition, the photocatalytic activities of Ce–TiO_2/UHMWPE were evaluated by the photocatalytic degradation of a methyl orange (MO) aqueous solution under UV irradiation.

EXPERIMENTAL

Materials

All of the chemicals used in the experiments were analysis grade and were used without further purification. Titanium tetrabutoxide [$Ti(OC_4H_{9-n})_4$; 98%, Sinopharm Chemical Reagent Co., Ltd., Shanghai, China] was used as a titanium precursor. Cerium nitrate hexahydrate [$Ce(NO_3)_3{\cdot}6H_2O$; 99%, Sinopharm Chemical Reagent Co. Ltd., Shanghai, China] was used as a Ce source. Anhydrous ethanol (C_2H_5OH; 99.7%, Jiuyi Chemical Reagent Co., Ltd., Shanghai, China), acetic acid (HAc, 99.5%, Shanghai Chemical Reagent Co., Ltd., Shanghai, China) and nitric acid (HNO_3; 70%) were used as solvents. UHMWPE powder, with an average particle size of 60 μm, a molecular weight of 3×10^6, and a density of 0.935 g/cm^3, was provided by Beijing No.2 Auxiliary Agent Plant (Beijing, China). Sodium chloride (NaCl), with an average particle size of 45 μm, was used as a channeling agent.

Preparation of the Ce–TiO_2/UHMWPE Porous Composites

Synthesis of the Ce–TiO_2 Nanoparticles. The cerium-ion-doped titanium dioxide (Ce–TiO_2) catalysts were prepared via a sol–gel route that was reported previously.[22] $Ti(OC_4H_{9-n})_4$ (10 mL) was diluted in 40 mL of absolute ethanol under magnetic stirring, and 20 mL of acetic acid was added dropwise into the $Ti(OC_4H_{9-n})_4$ solution. This was followed by the addition of 1 mL of HNO_3 and a specific amount of $Ce(NO_3)_3$. The molar proportion of Ce in TiO_2 was varied as 0, 0.5, 1.0, 1.5, 2.0, and 2.5%; the samples with these proportions were named TiO_2, TiO_2–Ce0.5, TiO_2–Ce1.0, TiO_2–Ce1.5, TiO_2–Ce2.0, and TiO_2–Ce2.5, respectively. The resulting transparent colloidal suspension was stirred and calcined to form the Ce–TiO_2 powder.

Preparation of the Ce–TiO_2/UHMWPE Porous Composites. The prepared Ce–TiO_2 nanoparticles were surface-modified by a silane coupling agent (KH570), as described in detail previously.[23] KH570 (5 mL), anhydrous ethanol (100 mL), and 40 mg of Ce–TiO_2 were added to a three-necked flask equipped with a magnetic stirrer at 80°C for 6 h. The functionalized Ce–TiO_2 solution was obtained. Then, the UHMWPE particles were added, and a similar step was repeated. Finally, the solution was filtered and washed with deionized water until the liquid became neutral, and the final products were the Ce–TiO_2 and UHMWPE hybrid particles.

The Ce–TiO_2 and UHMWPE complex particles were treated at 150°C for 2 h to make the UHMWPE partially melt so that the nanoparticles could adhere to the surface of UHMWPE. The mixture particles and NaCl powders were pressed into a stainless mold at 10 MPa of pressure and heated to 180°C for 6 h; then, the mold was cooled to room temperature, and NaCl was removed in deionized water. Finally, the resulting Ce–TiO_2/UHMWPE porous composite was obtained. To examine the effect of its content on the properties of the materials, the volume proportions of Ce–TiO_2 in the compositions were varied as follows: 0.5, 1, 2, 4, 5, and 8 vol %. The concentration of NaCl was kept at 40 vol %. For comparison, a pure UHMWPE porous sample was also prepared without the addition of Ce–TiO_2 under the same chemical conditions. The details of the porous composites recipes are shown in Tables I and II.

Characterization

Scanning electron microscopy (SEM; Hitachi S-4700, Tokyo, Japan) was used to observe the morphologies of the composite materials. The surface functional groups of Ce–TiO_2 were analyzed by Fourier transform infrared (FTIR) spectroscopy (Nicolet Magna IR550) to estimate the modification effect. The porous structure was investigated via mercury porosimetry. To study the UV-induced photocatalytic stability, a UV light (300-W Hg lamp, Philips, Suzhou, China) and UV–visible (UV–vis) spectrometer (PerkinElmer Lambda 900 UV–vis/near infrared spectrometer, Waltham, MA) were used. The hydrophilicities of the surfaces were characterized by water contact angle measurements with a FACE CA-X instrument. All contact angles were the mean value of five measurements on different parts of the porous composites surface.

Photocatalytic Reactions

Before the reaction, the samples were kept in methylene orange solution (250 mL, 20 mg/L) in the dark for 1 h to reach adsorption/desorption equilibrium. Then, the solution was kept at 10 cm below the UV lamp and irradiated from above for 6 h. One 4 mL sample of MO solution was taken out per hour, and Ce–TiO_2 nanoparticles were separated from the dye solution with centrifugation at 8000 rpm for 6 min. Then, the clear solution was measured with the UV–vis spectrometer at a wavelength of 500 nm. The degradation rate was calculated by the following equation:[24]

Table II. Specifications of the Samples with Different Concentrations of TiO_2–1.5Ce Particles

Porous material	Volume proportion of TiO_2–1.5Ce in the composition (vol %)
P_0	0
P_1	0.5
P_2	1.0
P_3	2.0
P_4	4.0
P_5	8.0

Applied Polymer SCIENCE

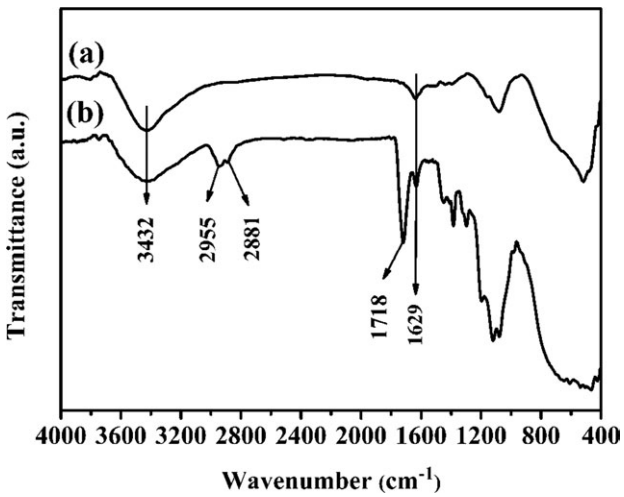

Figure 1. FTIR spectra of the (a) bare Ce–TiO_2 particles and (b) KH570 modified Ce–TiO_2.

$$D_r = \frac{C_0 - C_t}{C_0} \times 100\% \quad (1)$$

where C_0 and C_t are the initial concentration and the concentration after radiation of MO, respectively, and D_r is the degradation rate of MO.

Filtration Performance

The water flux values of all of the samples were determined under 1 MPa of pressure at room temperature in cross-flow filtration with 0.5 g/L bovine serum albumin (BSA) powder dissolved in deionized water. The flux (J) values for the UHMWPE and Ce–TiO_2/UHMWPE samples were calculated by the following equation:[25]

$$J = \frac{V}{AT} \quad (2)$$

where V, A, and T are the volume of water collected, the surface area of the sample, and the time taken to collect the water, respectively.

RESULTS AND DISCUSSION

FTIR Analysis

To improve the compatibility between the Ce–TiO_2 nanoparticles and the UHMPHE matrix, the Ce–TiO_2 nanoparticles were modified with KH570, and the modification effects were characterized by FTIR spectroscopy. Figure 1 shows the FTIR spectroscopy of Ce–TiO_2 before and after the modification by KH570. Both curves exhibited peaks around 3432 and 1629 cm^{-1}, which corresponded to the stretching and bending vibrations of hydroxyl groups. Interestingly, the two hydroxyl characteristic peaks were strengthened largely in the spectrum of the modified Ce–TiO_2; this indicated that the surface activity was improved.[16] The strong absorption band between 1000 and 500 cm^{-1} were the characteristic peaks of the Ti—O and Ti—O—Ti bands.[24,26] Notably, the spectrum of the modified Ce–TiO_2 showed some new peaks at 2955, 2881, and 1718 cm^{-1}; these were assigned to the absorbance of —CH_3—, —CH_2—, and —C=O— in KH570, respectively. The appearance of these new peaks indicated that the Ce–TiO_2 nanoparticles were successfully modified by KH570.

SEM Analysis

Figure 2 shows the SEM images of the original UHMWPE particles before and after they were coated with Ce–TiO_2. As shown in Figure 2(a), the original polymer particles had a smooth surface. Comparatively, after they were covered with small globular Ce–TiO_2 particles, the polymer particles had a rougher surface. Ce–TiO_2 particles were uniformly coated around the polymer surface after they were treated with the silane coupling agent [Figure 2(b)].

The morphologies of the UHMWPE and Ce–TiO_2/UHMWPE composites are shown in Figure 3. Compared with that of the bare UHMWPE porous sample, the morphology of the composites filled with Ce–TiO_2 became rougher. It was clearly observed that the nanoparticles were strongly attached to the surface and the hole wall of UHMWPE. Because of the higher specific surface area of the nanoparticles, they had more contact area with the polymer matrix; this was beneficial to the expansion of the photocatalytic reaction surface and the effective improvement of the photocatalytic activity.

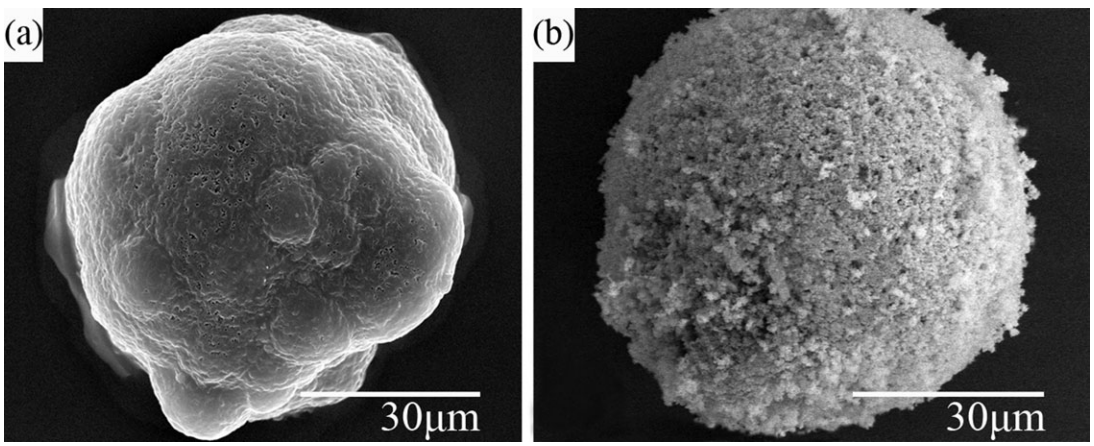

Figure 2. Surface SEM micrograph of the (a) pure UHMWPE particles and (b) UHMWPE particles coated by Ce–TiO_2 nanoparticles.

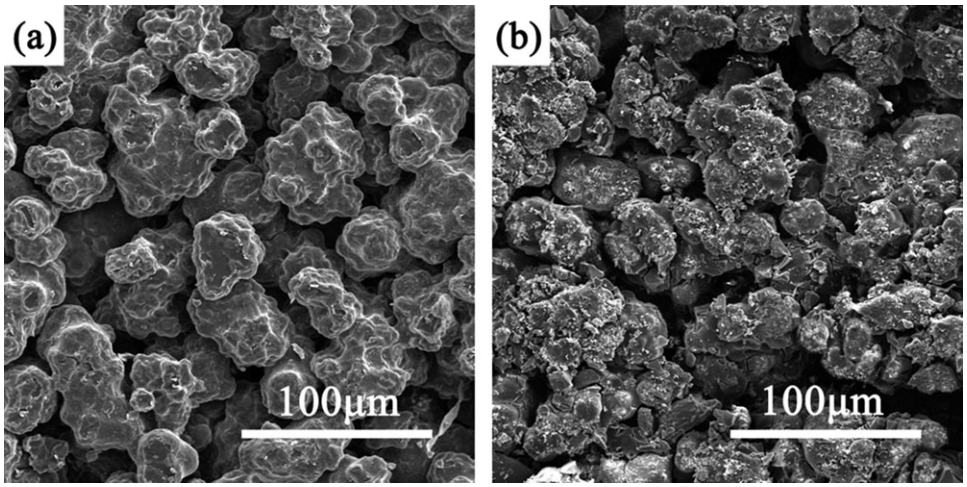

Figure 3. SEM analyses of the porous structure of the (a) pure UHMWPE porous materials and (b) Ce–TiO_2/UHMWPE composite materials.

UV–vis Diffuse Reflectance Spectra

The UV–vis spectra of the TiO_2/UHMWPE (sample C_0) and Ce–TiO_2/UHMWPE (sample C_5) samples are presented in Figure 4. The results demonstrate that C_0 had no absorption in the visible region (>375 nm) and that C_5 exhibited a redshift of the absorption edge and a significant enhancement of optical absorption between 375 and 450 nm. In fact, enhanced absorption in the visible region for Ce-doped TiO_2 has been reported.[22,27] The absorptions in the UV region of C_0 and C_5 were due to a transfer process from the 2p orbitals of O^{2-} ions to the t_{2g} orbitals of the Ti^{4+} ions in the composites.[28] Meanwhile, C_5 showed a spectral response in the visible region for the presence of Ce, which showed a photosentisizing effect.

Photocatalytic Activity

Figure 5 shows the degradation rate of MO by the composites. It is clearly shown that all of the samples containing Ce–TiO_2 had a higher degradation rate than the ones with TiO_2. The degradation rate of MO increased with increasing Ce content in the composites. However, when the concentration reached 2.0%, the degradation rate started to decrease. This tendency was in good agreement with a previous study by Li et al.[22] With an appropriate content of Ce (1.5%), the CeO_2 particles were well dispersed on the TiO_2 surface, and Ce^{4+} could act as electron–hole separation centers to capture the photogenerated electrons. A further increase in the Ce concentration led to the agglomeration of CeO_2 nanoparticles. The trap center could become the recombination center of photogenerated electron–hole pairs.

Photocatalytic Degradation

The MO discoloration of six types by porous composites under UV light is shown in Figure 6. The samples had similar adsorptions in the dark for 1 h; this illustrated that the adsorption ability was not the main factor influencing the photodegradation rate. Figure 6(a) shows that the MO discoloration curve of P_0 did not change significantly because of the absence of the Ce–TiO_2 catalyst. Interestingly, P_3 showed the best photocatalytic activity compared to the others. This could be explained by the following mechanisms: (1) under UV light irradiation, the excited TiO_2 nanoparticles produced electron–hole pairs,

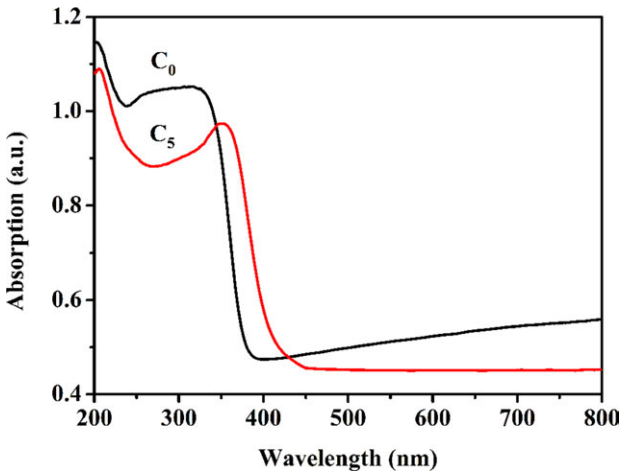

Figure 4. UV–vis diffuse reflectance spectra of C_0 and C_5. [Color figure can be viewed in the online issue, which is available at wileyonlinelibrary.com.]

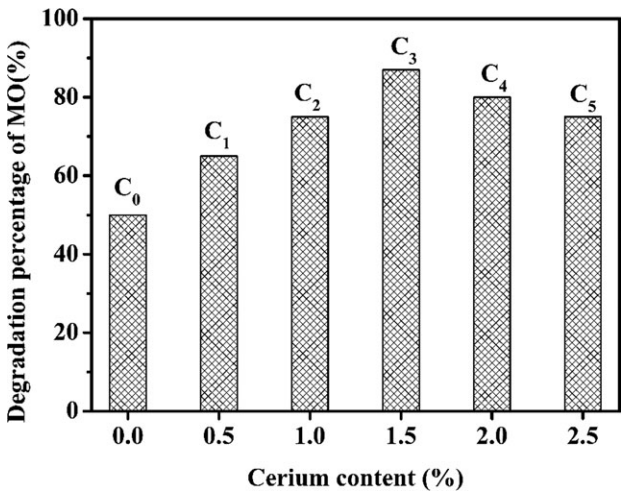

Figure 5. Photodegradation of MO with different samples under UV irradiation for 6 h.

Applied Polymer SCIENCE

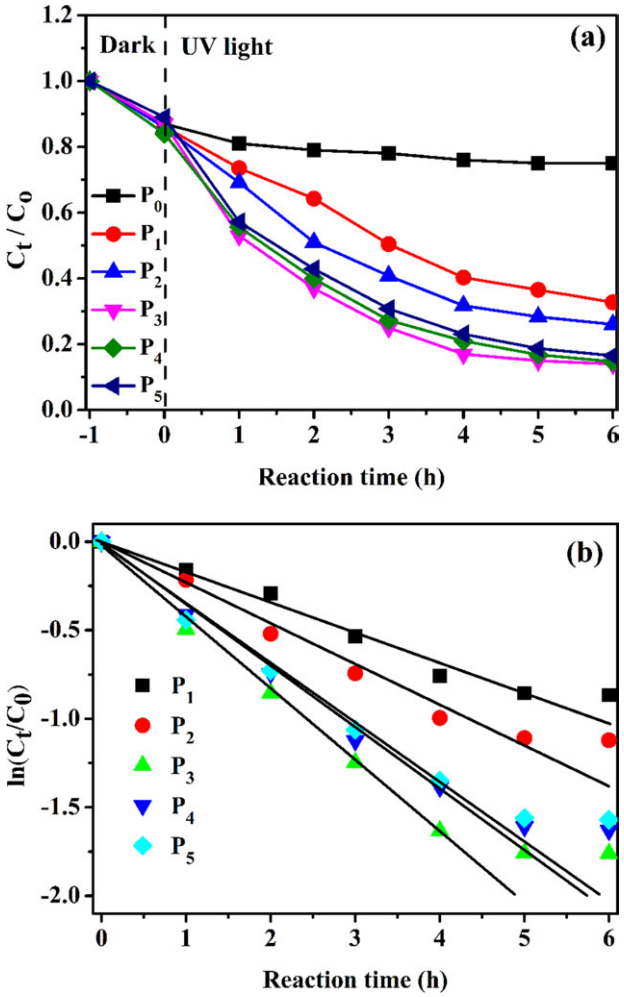

Figure 6. (a) MO discoloration with UV light in the presence of different samples and (b) first-order kinetic treatment. [Color figure can be viewed in the online issue, which is available at wileyonlinelibrary.com.]

and when they arrived at the surface, they were trapped by Ce, (2) the Ce–TiO_2 catalyst had many more surface hydroxyl groups because of its large surface area, and (3) the coupling agent dramatically increased the surface reaction sites of nanoparticles and gave the inorganic particles better dispersion and adhesion onto the surface of the polymer matrix. Therefore, the photocatalytic activity of sample P_3 improved remarkably.

The photocatalytic activity of the porous composites increased gradually with increasing Ce–TiO_2 nanoparticle concentration. This was attributed to the improvement in the removal and oxidation efficiency of the UHMWPE MO adsorption capability.[29] Meanwhile, the surface roughness of the composite samples was higher than that of the pure UNMWPE porous materials; this was favorable for the absorption and decomposition of the pollutant under UV irradiation. However, when the concentration of Ce–TiO_2 reached 4%, the composites showed a low discoloration rate constant obtained from the slope of the $\ln(C_t/C_0)$ plots versus the time plots [Figure 6(b)].[30] This was due to the agglomeration of the Ce–TiO_2 nanoparticles, and they did not effectively attach onto the UHMWPE matrix and were deposited at the bottom of the reactor (the nonilluminated part).

Photocatalytic Mechanism Discussion

On the basis of the results of photocatalytic tests, the photocatalytic process under UV light irradiation could be inferred as follows. TiO_2 particles absorbed light at wavelengths below 390 nm to generate electron–hole pairs in the conduction band (CB) and valence band (VB). However, the electron–hole pairs recombined quickly. In the presence of Ce, the recombination of electron–hole pairs was limited, and the subsequent reactions caused by the electrons and holes could be effectively enhanced. Then, the special electron configuration of Ce played an important role in the reaction process. Lanthanide ions, acting as a Lewis acid, are superior to oxygen molecules (O_2) in their capability of trapping CB electrons.[28,31] The electrons could be captured by Ce^{4+} and then be transferred to the O_2 adsorbed on the TiO_2 surface to form superoxide anion radicals ($^{\bullet}O^{-2}$). Ce has a high oxygen transportation and storage capacity, and the excited electrons could be more easily transfer to O_2 and form more superoxide anion radicals. At the same time, the positively charged hole (h^+) could react with H_2O to generate $^{\bullet}OH$. The superoxide radical ion ($^{\bullet}O^{-2}$) and hydroxyl radical $^{\bullet}OH$ are two important reactive oxygen species for the photocatalytic degradation of MO.[32] The whole process is displayed in Figure 7.

Permeability of the UHMWPE and Ce–TiO_2/UHMWPE Samples

Figure 8 provides the flux behavior of the original and Ce–TiO_2-deposited UHMWPE samples. The flux of all of the samples decreased sharply at the beginning of BSA solution filtration and decreased gradually. Notably, the flux values became stable up to 120 min. Unexpectedly, the initial flux value of P_0 was high and declined dramatically compared with the samples modified by Ce–TiO_2. These results show that the antifouling properties of the Ce–TiO_2-deposited samples were expressed more effectively than those of the unmodified sample. Photodegradation accompanied by filtration occurred, O_2 turned into $^{\bullet}O^{-2}$, and an oxygen vacancy was produced on the surface of the polymer matrix. Water molecules occupying the oxygen vacancies could adsorb OH groups appearing on the surface of the composites, and this decreased the contact angle and increased the hydrophilicity of the composites.[33] Hence, water flowed easily through the porous materials. Additionally,

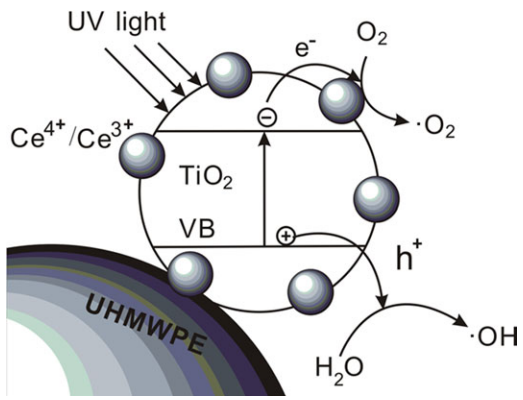

Figure 7. Pathway of MO photodegradation by the Ce–TiO_2/UHMWPE composites under UV irradiation. [Color figure can be viewed in the online issue, which is available at wileyonlinelibrary.com.]

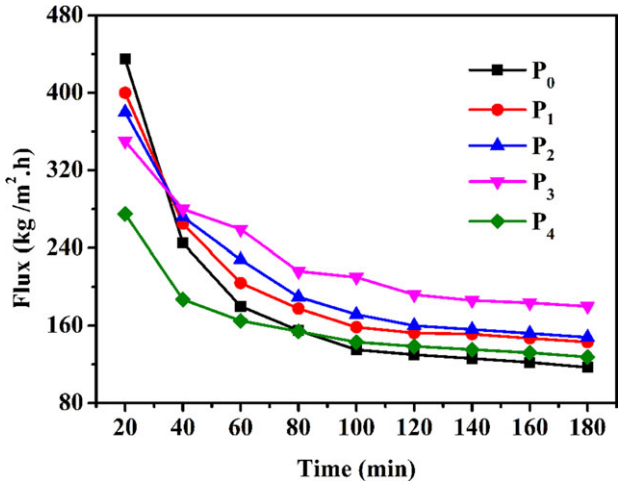

Figure 8. Flux behavior of the pure UHMWPE and the Ce–TiO_2-deposited UHMWPE porous composites in the BSA solution. [Color figure can be viewed in the online issue, which is available at wileyonlinelibrary.com.]

the fouling mitigation effect was gradually enhanced by the increase in Ce–TiO_2 concentration up to 2.0 vol %. A further increase in the Ce–TiO_2 concentration reduced the flux because of the formation of blockages in the surface and pores of the polymer matrix.

CONCLUSIONS

Through effective surface modification of the Ce–TiO_2 nanoparticles, the nanoparticles were uniformly dispersed on the surface of the UHMWPE matrices. The degradation rate of MO showed that the photocatalytic activity of the Ce–TiO_2/UHMWPE composites could be controlled by the Ce–TiO_2 nanoparticle content. The Ce–TiO_2/UHMWPE composites showed a higher photocatalytic activity than TiO_2/UHMWPE because the doped Ce in TiO_2 efficiently expanded the photoresponse region and eliminated the recombination of electron–hole pairs. In addition, the composites possessed excellent permeability in wastewater. The development of Ce–TiO_2/UHMWPE nanoparticle composites can lead to an ecofriendly filter and the disposal of organic pollutants in wastewater treatment.

ACKNOWLEDGMENT

This work was supported by the National Engineering Laboratory of Modern Silk (project number SS115801) and the A Project Academic Program Development of Jiangsu Higher Education Institutions.

REFERENCES

1. Yang, G. W.; Han, H. Y.; Du, C. Y.; Luo, Z. H.; Wang, Y. *J. Polymer* **2010**, *51*, 6193.
2. Maximous, N.; Nakhla, G.; Wan, W.; Wong, K. *J. Membr. Sci.* **2009**, *341*, 67.
3. Hartmann, M.; Kullmanna, S.; Keller, H. *J. Mater. Chem.* **2010**, *20*, 9002.
4. Fouad, H. *J. Appl. Polym. Sci.* **2009**, *118*, 17.
5. Aydinli, B.; Tincer, T. *J. Appl. Polym. Sci.* **2013**, *127*, 1077.
6. Ruan, S. L.; Gao, P.; Yu, T. X. *Polymer* **2006**, *47*, 1604.
7. Yu, L. Y.; Shen, H. M.; Xu, Z. L. *J. Appl. Polym. Sci.* **2009**, *113*, 1763.
8. Su, Y. L.; Cheng, W.; Li, C.; Jiang, Z. Y. *J. Membr. Sci.* **2009**, *329*, 246.
9. Cornelissen, E. R.; Vrouwenvelder, J. S.; Heijman, S. G. J.; Viallefont, X. D.; Van Der Kooij, D.; Wessels, L. P. *J. Membr. Sci.* **2007**, *287*, 94.
10. Tian, G. H.; Fu, H. G.; Jing, L. Q.; Xin, B. F.; Pan, K. *J. Phys. Chem. C* **2008**, *112*, 3083.
11. Liu, X. L.; Gao, Y. F.; Cao, C. X.; Luo, H. J.; Wang, W. Z. *Langmuir* **2010**, *26*, 7671.
12. Pan, J. H.; Zhao, X. S.; Lee, W. I. *Chem. Eng. J.* **2011**, *170*, 363.
13. Lee, K.; Lee, S. *J. Appl. Polym. Sci.* **2012**, *124*, 4038.
14. Li, J. F.; Xu, Z. L.; Yang, H.; Yu, L. Y.; Liu, M. *Appl. Surf. Sci.* **2009**, *255*, 4725.
15. Madaeni, S. S.; Zinadini, S.; Vatanpour, V. *J. Membr. Sci.* **2011**, *380*, 155.
16. Magalhães, F.; Lago, R. M. *Sol. Energy* **2009**, *83*, 1521.
17. Gole, J. L.; Stout, J. D.; Burda, C.; Lou, Y. B.; Chen, X. B. *J. Phys. Chem. B* **2004**, *108*, 1230.
18. Montazer, M.; Behzadnia, A.; Moghadam, M. B. *J. Appl. Polym. Sci.* **2012**, *125*, 356.
19. Katoh, R.; Furube, A.; Yamanaka, K.; Morikawa, T. *J. Phys. Chem. Lett.* **2010**, *1*, 3261.
20. Sauthier, G.; Pérez del Pino, A.; Figueras, A.; György, E. *J. Am. Ceram. Soc.* **2011**, *94*, 3780.
21. Gao, J.; Yang, M.; Lei, J. X. *J. Appl. Polym. Sci.* **2012**, *124*, 5286.
22. Li, F. B.; Li, X. Z.; Hou, M. F.; Cheah, K. W.; Choy, W. C. H. *Appl. Catal. A* **2005**, *285*, 181.
23. Yao, Q. Z.; Zhou, Y. M. *J Inorg. Organomet. Polym.* **2009**, *19*, 215.
24. Wang, D.; Zhang, J.; Luo, Q. Z.; Li, X. Y.; Duan, Y. D.; An, J. *J. Hazard Mater.* **2009**, *169*, 549.
25. Oh, S. J.; Kim, N.; Lee, Y. T. *J. Membr. Sci.* **2009**, *345*, 13.
26. Comparelli, R.; Fanizza, E.; Curri, M. L.; Cozzoli, P. D.; Mascolo, G.; Passino, R.; Agostiano, A. *Appl. Catal. B* **2005**, *55*, 81.
27. Tong, T. Z.; Zhang, J. L.; Tian, B. Z.; Chen, F.; He, D. N.; Anpo, M. *J. Colloid Interface Sci.* **2007**, *315*, 382.
28. Xie, Y. B.; Yuan, C. W. *Appl. Catal. B* **2003**, *46*, 251.
29. Magalhães, F.; Flávia, C. C. M.; Rochel, M. L. *Desalination* **2011**, *276*, 266.
30. Kasanen, J.; Salstela, J.; Suvanto, M.; Pakkanen, T. T. *Appl. Surf. Sci.* **2001**, *258*, 1738.
31. Coronado, J. M.; Martínez-Arias, A.; Conesa, J.; Soria, J. *J. Photochem. Photobiol. A* **2002**, *150*, 213.
32. Zhang, H.; Zong, R. L.; Zhao, J. C.; Zhu, Y. F. *Environ. Sci. Technol.* **2008**, *42*, 3803.
33. Rahimpour, A.; Jahanshahi, M.; Mollahosseini, A.; Rajaeian, B. *Desalination* **2012**, *285*, 31.